

19

Creeping flow

Viscosity may be so large that a fluid only flows with difficulty. Heavy oils, honey, even tight crowds of people, show insignificant effects of inertia, and are instead dominated by internal friction. Such fluids do not make spinning vortices or become turbulent, but rather ooze or creep around obstacles. Fluid flow which is dominated by viscosity is quite appropriately called creeping flow.

Since there is no absolute meaning to “large” viscosity, creeping flow is more correctly characterized by the Reynolds number being small, $Re \ll 1$. Creeping flow may occur in any fluid, as long as the typical velocity and geometric extent of the flow combine to make a small Reynolds number. Blood flowing through a microscopic capillary can be as sluggish as heavy oil. Tiny organisms like bacteria live in air and water like ourselves, but their’s is a world of creeping and oozing rather than whirls and turbulence, and movement requires special devices, for example oar-like cilia or whip-like flagella [36]. Some bacteria have even mounted a rotating helical tail in a journal bearing (the only one known to biology), which like a corkscrew allows them to advance through the thick fluid that they experience water to be. A spermatozoan pushes forward like a slithering snake in the grass by undulating its tail.

In this chapter we shall study creeping flow around moving bodies far from containing boundaries. For any creature in creeping flow, the most important quantity is the fluid’s resistance against motion, also called *drag*. The drag on a body has two components of comparable magnitude in creeping flow, one being *skin drag* from viscous friction between the fluid and the body, and the other *form drag* from the variations in fluid pressure across the body. The same contact forces may also produce *lift* orthogonally to the direction of motion, but in creeping flow lift is of roughly the same order of magnitude as drag. A tiny creature that already must overcome a drag many times its weight in order to move freely has no problem with flying. That’s why bacteria don’t have wings.

19.1 Steady incompressible creeping flow

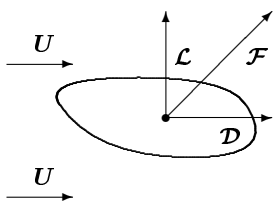
Leaving out the time dependence and the advective terms, we obtain from the Navier-Stokes equations (17-28) the following equations for steady incompressible creeping flow

$$\begin{cases} \eta \nabla^2 \mathbf{v} = \nabla p^* , \\ \nabla \cdot \mathbf{v} = 0 , \end{cases} \quad (19-1)$$

where p^* is the effective pressure (??). The condition for using this approximation is that the Reynolds number (17-20) is small, $\text{Re} \ll 1$.

Creeping flow is mathematically (and numerically) much easier to handle than general flow because of the absence of non-linear (advective) terms that tend to spontaneously break the natural symmetry of the solutions in time as well as space (with turbulence as the extreme result). Furthermore, the linearity of the equations makes it possible to express solutions to more complicated flow problems as linear superpositions of simpler solutions. Creeping flow is also called Stokes flow.

Estimate of forces on a moving body



The total contact force \mathcal{F} is composed of lift \mathcal{L} and drag \mathcal{D} .

Suppose a body is moving through a fluid with a steady velocity U far from containing boundaries. As pointed out before, this situation does *not* correspond to steady flow. Cruising through the fluid, the moving body creates a temporary disturbance that disappears again some time after the body has passed a fixed observation point. But seen from the body, the fluid appears to move in a steady pattern which at sufficiently large distances becomes a uniform flow of magnitude U . Newtonian relativity guarantees that these situations are physically equivalent, so that we may use the creeping flow equations (19-1).

The only way the fluid can influence a solid body is through contact forces acting on its surface. It is convenient to resolve the total contact force

$$\mathcal{F} = \mathcal{D} + \mathcal{L} \quad (19-2)$$

into two vector components. The first \mathcal{D} is called the *drag* and acts in the direction of the asymptotic flow, $\mathcal{D} = \mathcal{D} \mathbf{e}_U$ where $\mathbf{e}_U = \mathbf{U}/U$. The other \mathcal{L} is called the *lift* and acts orthogonally to the direction of asymptotic flow, so that $\mathcal{L} \cdot \mathbf{e}_U = 0$.

We shall think of the body as having a non-exceptional roughly globular shape with diameter L and assume that the Reynolds number $\text{Re} \approx \rho U L / \eta$ satisfies $\text{Re} \ll 1$. Since the pressure only appears in (19-1) in the combination p^*/η , and since the boundary conditions do not involve the pressure, the velocity field cannot depend on η , but only on the asymptotic velocity U and on the shape and orientation of the body. The linearity further guarantees that the velocity field \mathbf{v} and p^*/η must be proportional to U everywhere. The velocity gradients

near the surface must therefore be of magnitude $|\nabla \mathbf{v}| \sim U/L$ so that the shear stress becomes $\sigma \sim \eta U/L$. Multiplying with the surface area of the body $\sim L^2$ we obtain an estimate of the skin drag,

$$\mathcal{D}_{\text{skin}} = f_{\text{skin}} \eta U L, \quad (19-3)$$

with an unknown dimensionless prefactor f_{skin} of order unity, determined by the detailed geometry of the body. We may similarly estimate the pressure gradient near the surface from (19-1) to be $|\nabla p^*| \approx \eta U/L^2$, and multiplying with the length L of the body, we estimate the pressure variations over the body to be of the same size as the shear stress, $|\Delta p^*| \sim \eta U/L$. Multiplying as before with the surface area L^2 , the estimate of the form drag becomes of the same order of magnitude as skin drag,

$$\mathcal{D}_{\text{form}} = f_{\text{form}} \eta U L, \quad (19-4)$$

but in general it has another geometric prefactor.

The total drag is the sum of skin and form drag, and becomes of order of magnitude $\mathcal{D} \sim \eta U L$. Lift is produced by the same contact forces as drag and is also of this magnitude, $\mathcal{L} \sim \eta U L$, but the geometric prefactor is here strongly dependent on the orientation of the body with respect to the direction of flight. Furthermore, near a solid boundary lift can grow much larger than drag and may keep the body away from the boundary. This is in fact the secret behind lubrication (see the following chapter).

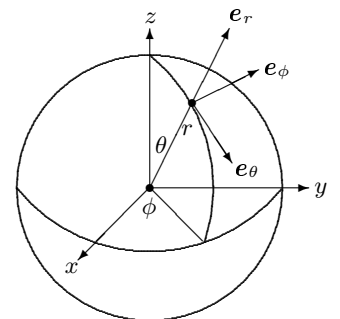
19.2 Stokes' solution for a sphere

A solid sphere moving at constant speed through a viscous fluid is the centerpiece of steady creeping flow (Stokes, 1851). The solution may be worked out starting from the field equations (19-1) and the boundary conditions (see problem 19.8), but even if the details of obtaining the solution are a bit complicated, the result is fairly simple. In spherical coordinates with polar axis in the direction of \mathbf{U} , the resulting flow is given by

$$\boxed{\begin{aligned} v_r &= \left(1 - \frac{3a}{2r} + \frac{1}{2} \frac{a^3}{r^3}\right) U \cos \theta \\ v_\theta &= -\left(1 - \frac{3a}{4r} - \frac{1}{4} \frac{a^3}{r^3}\right) U \sin \theta \\ v_\phi &= 0 \end{aligned}}, \quad (19-5)$$

where a is the radius of the sphere. The effective pressure

$$p^* = -\frac{3}{2} \frac{\eta a}{r^2} U \cos \theta \quad (19-6)$$



Spherical coordinates and their tangent vectors.

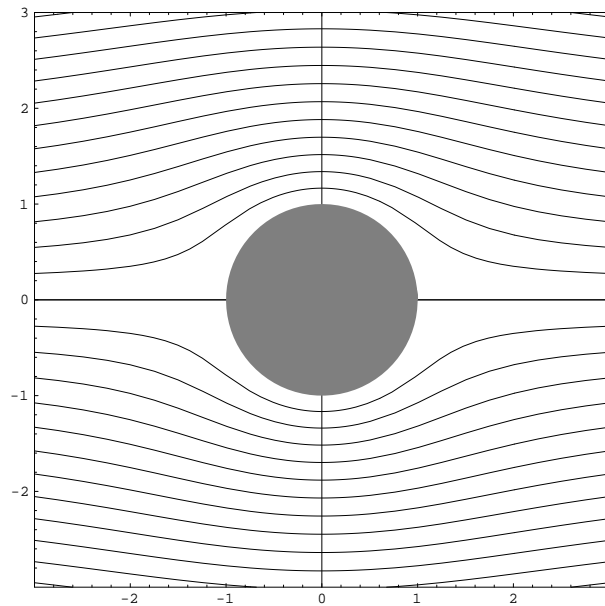


Figure 19.1: *Creeping flow around the unit sphere. Stream lines have been obtained by numeric integration of eq. (14-15) starting equidistantly at $z = -100$ to avoid problems of long range terms (see problem 19.6 for how to obtain the streamlines)*

is forward-backwards asymmetric, such that the pressure is highest on the part of the sphere that turns towards the incoming fluid (at $\theta = \pi$). This asymmetry is in marked contrast with the potential flow solution (15-62) for a sphere where the symmetry of the pressure gives rise to d'Alembert's paradox.

It is not particularly difficult to demonstrate from the spherical Laplacian (2-75) that the Stokes flow field is indeed a solution to the creeping flow equations. The vanishing of the azimuthal component v_ϕ is a consequence of the symmetry of the problem, and implies that there is no lift. At the surface of the sphere the velocity field vanishes as it should, and at infinity it approaches that of the uniform flow with velocity U in the z -direction, having $U_r = U \cos \theta$ and $U_\theta = -U \sin \theta$. Notice that the flow pattern is independent of the viscosity η of the fluid, and that the pressure is proportional to the viscosity. This is, as discussed above, common for creeping flow problems where the boundary conditions do not directly involve the pressure but only the velocity field.

Surface stresses

Let us first calculate the normal and shear stress tensor components. Using that $\sigma_{ij} = -p\delta_{ij} + \eta(\nabla_i v_j + \nabla_j v_i)$ we find the radial stress

$$\sigma_{rr} = -p + 2\eta \frac{\partial v_r}{\partial r} = \frac{3}{2} \frac{a}{r^2} \left(3 - 2 \frac{a^2}{r^2} \right) \eta U \cos \theta .$$

For the shear stress we get similarly

$$\begin{aligned}\sigma_{\theta r} &= \eta(\mathbf{e}_\theta)_i(\nabla_i v_j + \nabla_j v_i)(\mathbf{e}_r)_j = \eta \left(\frac{1}{r} \frac{\partial \mathbf{v}}{\partial \theta} \cdot \mathbf{e}_r + \frac{\partial \mathbf{v}}{\partial r} \cdot \mathbf{e}_\theta \right) \\ &= \eta \left(\frac{1}{r} \frac{\partial v_r}{\partial \theta} - \frac{v_\theta}{r} + \frac{\partial v_\theta}{\partial r} \right) = \eta \frac{1}{r} \left(2 - 3 \frac{a}{r} - \frac{1}{2} \frac{a^3}{r^3} \right) U \sin \theta.\end{aligned}$$

At the surface of the sphere, $r = a$, the two stress components become

$$\sigma_{rr}|_{r=a} = \frac{3}{2a} \eta U \cos \theta, \quad (19-7a)$$

$$\sigma_{\theta r}|_{r=a} = -\frac{3}{2a} \eta U \sin \theta, \quad (19-7b)$$

from which we get the stress vector

$$\boldsymbol{\sigma}|_{r=a} = \boldsymbol{\sigma} \cdot \mathbf{e}_r|_{r=a} = \mathbf{e}_r \sigma_{rr} + \mathbf{e}_\theta \sigma_{\theta r} = \frac{3}{2a} \eta U. \quad (19-8)$$

Surprisingly, it is of constant magnitude and points everywhere on the surface in the direction of the asymptotic flow.

Stokes law

The total force is obtained by multiplying the constant stress vector with the area $4\pi a^2$ of the sphere,

$$\boxed{\mathcal{F} = 6\pi\eta a U}. \quad (19-9)$$

This is the famous *Stokes law* from 1851. The symmetry of the sphere could have told us in advance that the force would be parallel with the velocity, because there is no geometric direction defined that a lift could take. The form was already predicted in (19-3) with a geometric prefactor $f = 3\pi$, taking $L = 2a$ to represent the size of the body. A quick calculation reveals that two thirds of the total is skin drag and one third is form drag (problem 19.5).

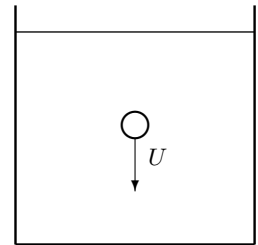
Falling sphere

Although Stokes law has been derived in the rest system of the sphere, it is also valid in the rest system of the asymptotic fluid. The terminal velocity of a falling solid sphere may be obtained by equating the force of gravity (minus buoyancy) with the Stokes drag

$$(\rho_{\text{sphere}} - \rho_{\text{fluid}}) \frac{4}{3} \pi a^3 g_0 = 6\pi\eta a U \quad (19-10)$$

where g_0 is the gravitational acceleration. Solving for U we find

$$U = \frac{2}{9} \left(\frac{\rho_{\text{sphere}}}{\rho_{\text{fluid}}} - 1 \right) \frac{a^2 g_0}{\nu} \quad (19-11)$$



Sphere falling through viscous fluid at constant terminal speed U .

where $\nu = \eta/\rho_{\text{fluid}}$ is the kinematic viscosity.

Example 19.2.1: Sand grains of diameter 0.1 mm and density 2.5 times that of water float towards the bottom of the sea with a terminal velocity of 1 cm s^{-1} , as calculated from Stokes' law. The corresponding Reynolds number is about 1, which is at the limit of the region of validity of Stokes' law.

Conversely, in the *falling sphere viscometer* this equation may be used to determine the viscosity ν from a measurement of the terminal velocity for a sphere of known radius.

One may also, as Millikan did in his famous electron charge experiment (1913), determine the radius of a falling sphere (an oil drop) from a measurement of the terminal velocity, provided the viscosity of the fluid is known. In Millikan's experiment the oil drops were charged and could be made to hover or fall in the field of gravity as slowly as desired by means of an electric field of suitable strength. Knowing the radius, the electric force on an oil drop could be compared to gravity, allowing the charge to be determined. The viscosity of air was determined by Couette viscometer measurements (section 18.10). At that time, there was actually an error in the viscosity of air deriving from the failure to take into account the effects of the end caps of the Couette viscometer, an error first corrected in 1930. Millikan also showed that it was necessary to include corrections to Stokes law for the internal motion of the oil in the tiny drops.

Robert A. Millikan (1868 - 1953). *American physicist. Awarded the Nobel prize in 1923 for the determination of the charge of the electron.*

Limits to Stokes flow

Stokes law has been derived under the assumption of creeping flow, which can only be valid under the condition that the Reynolds number

$$\text{Re} = \frac{\rho 2aU}{\eta} \quad (19-12)$$

is small compared to unity, $\text{Re} \ll 1$. In the falling sphere viscometer where the terminal velocity is determined by the balance of forces (19-11), the Reynolds number varies as the third power of the radius. As long as the sphere is sufficiently small, the conditions for creeping flow can always be fulfilled.

The Reynolds number is, however, only a rough estimate for the ratio between advective and viscous terms in the Navier-Stokes equations for a particular geometry. Having obtained an explicit solution we may actually calculate this ratio everywhere in the fluid to see if it is indeed small. Close to the sphere, the velocity is very small because of the no-slip condition. Problems are only expected to arise at large distances, where the leading corrections to the uniform flow are provided by the a/r terms in the solution (19-5). At large distances the leading advective terms are of order

$$|\rho \mathbf{v} \cdot \nabla \mathbf{v}| \approx \rho U^2 \frac{a}{r^2}, \quad (19-13)$$

whereas the viscous terms become

$$|\eta \nabla^2 \mathbf{v}| \approx \eta U \frac{a}{r^3} . \quad (19-14)$$

So the ratio between inertial and viscous terms becomes

$$\frac{|\rho \mathbf{v} \cdot \nabla \mathbf{v}|}{|\eta \nabla^2 \mathbf{v}|} \approx \frac{\rho U r}{\eta} \approx \frac{r}{a} \text{Re} . \quad (19-15)$$

where Re is the global Reynolds number (19-12). As this expression grows with r , it follows that however small the Reynolds number may be, there will always be a distance $r \gtrsim a/\text{Re}$ where the advective terms begin to dominate. This clearly illustrates that the global Reynolds number is just a guideline, not a guarantee that creeping flow will occur everywhere in a system. Since any finite non-exceptional body at sufficiently large distances looks like a sphere, this problem must in fact be present in all creeping flows.

The slowly decreasing a/r terms in the solution (19-5) also indicate the influence of the containing vessel. The relative magnitude of these terms at the boundary of the vessel is estimated as $2a/D$ where D is the size of the vessel. In the falling sphere viscometer a 1% measurement of viscosity thus requires that the sphere diameter must be smaller than 1% of the vessel size. That can be hard to fulfil in highly viscous fluids where a measurable terminal speed demands rather large and heavy spheres.

19.3 Beyond Stokes' law

Stokes law has been derived in the limit of vanishing Reynolds number (19-12), and is empirically valid for $\text{Re} \lesssim 1$. For larger values of Re the simplicity of the problem nevertheless allows us to make a general analysis, as we did for turbulent pipe flow (section 18.7 on page 365), even if we cannot solve the Navier-Stokes equations.

Friction factor

Since the only parameters defining the problem are the radius a , the velocity U , the viscosity η and the density of the fluid ρ , we may for any Reynolds number write the drag on the sphere in the form of Stokes' law multiplied with a dimensionless factor f ,

$$\mathcal{D} = 6\pi\eta a U f(\text{Re}) , \quad (19-16)$$

The dimensionless factor can as indicated only depend on the dimensionless Reynolds number. It accounts for the deviations from Stokes law and is evidently anchored at unity for vanishing Reynolds number, *i.e.* $f(0) = 1$. We shall as for pipe flow call it the *friction factor*, although as mentioned above only 2/3 of the drag on the sphere is in fact due to friction (and 1/3 to the front-to-back pressure differences).

Drag coefficient

In the opposite limit, at large Reynolds number, the sphere literally plows its way through the fluid, leaving a wake of highly disturbed and turbulent fluid. The drag may be estimated from the rate of loss of momentum from the incoming fluid that is disturbed by the sphere. The incoming fluid carries a momentum density ρU and since the sphere presents a cross-sectional area $A = \pi a^2$ to the flow, we estimate the rate at which momentum impinges on the sphere to be $\rho U \cdot AU = \rho AU^2$. The drag at high Reynolds numbers is thus expected to grow with the square of the velocity (at subsonic speeds).

But the fluid in the wake trailing the sphere is not completely at rest, such that only a certain fraction of the incoming momentum will be lost. Empirically about 20% of the fluid momentum impinging on a sphere is lost to drag for $10^3 \lesssim \text{Re} \lesssim 10^5$. It is for this reason customary to define the dimensionless *drag coefficient*

$$C_D = \frac{\mathcal{D}}{\frac{1}{2}\rho\pi a^2 U^2}, \quad (19-17)$$

with a conventional factor 1/2 in the denominator. Empirically, the drag coefficient for a sphere is $C_D \approx 0.5$ in the interval $10^4 \lesssim \text{Re} \lesssim 2.5 \times 10^5$, implying that about 25% of the incoming fluid momentum is lost to drag.

Inserting the definition of the friction factor for a sphere (19-16) we find

$$C_D = \frac{24}{\text{Re}} f(\text{Re}) \quad (19-18)$$

for all Reynolds numbers. It is a matter of taste whether one prefers to describe the drag on a sphere by means of the drag coefficient or the friction factor. At small Reynolds numbers, it seems a bit pointless to use the drag coefficient, because it introduces a strong artificial variation $C_D \approx 24/\text{Re}$ for $\text{Re} \rightarrow 0$ without a corresponding strong variation in the physics (which is simply described by Stokes law). At large Reynolds numbers the drag coefficient becomes a constant, which is more convenient to use than the linearly rising friction factor.

Interpolation

One may join the regions of low and high Reynolds numbers by the simple interpolating expression

$$C_D = \frac{24}{\text{Re}} + \frac{5}{\sqrt{\text{Re}}} + 0.3 \quad (19-19)$$

The first term is Stokes' result and the last is a constant terminal form drag. The middle term may be understood as due to friction in a thin laminar boundary layer (see chapter 25) on the forward half of the sphere. There are a number of different formulas in the literature covering the same empirical data. As seen in fig. 19.2, this formula agrees decently with the measured values for all Reynolds numbers up to $\text{Re} \approx 10^4$, where the drag coefficient first rises to almost 0.5 and then drops sharply to about 0.1, after which it begins to rise again.

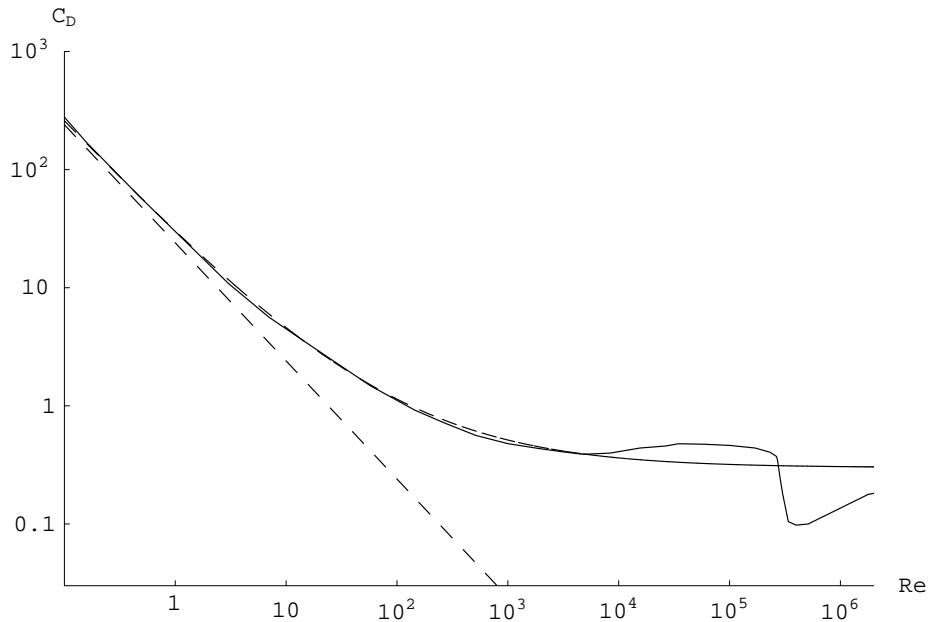
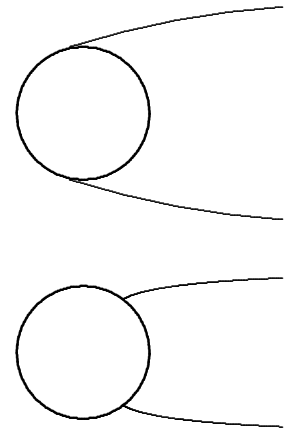


Figure 19.2: Sketch of the drag coefficient for a smooth ball (fully drawn). The dashed line corresponds to Stokes law $C_D = 25/Re$ and the dashed curve is the interpolation (19-19). The sharp drop (the “drag crisis”) at $Re = 2.5 \times 10^5$ signals the onset of turbulence in the boundary layer on the front half of the sphere and an accompanying shift in the shape of the trailing wake.

The drag crisis

This dramatic *drag crisis* is caused by a transition from laminar to turbulent flow in the boundary layer of the forward-facing half of the sphere. The transition is accompanied by a front-to-back shift in the separation point for the turbulent wake that trails the sphere. At a Reynolds number just beyond the drag crisis, the wake is narrower than before, entailing a smaller loss of momentum, *i.e.* drag. At still higher Reynolds numbers the drag coefficient regains part of its former magnitude, while at supersonic speeds it rises to around unity.

The Reynolds number at which the drag crisis sets in depends on the surface properties of the sphere. Roughness tends to facilitate the generation of a turbulent boundary layer and makes the onset of the drag crisis occur at lower Reynolds number. This is the deeper reason for manufacturing golf balls with surface dimples. A golf ball flying at a typical speed of 30 m s^{-1} has $Re \approx 1.6 \times 10^5$ which is below the drag crisis for a smooth ball, but not for a dimpled one. The lower drag on a dimpled ball permits it to fly longer for a given initial thrust. The seams of a tennis ball serve the same function, whereas a ping-pong ball is quite smooth. A ping-pong ball flying at 10 m s^{-1} has $Re \approx 5 \times 10^4$ which is probably too far below the drag crisis for dimples to work. Dimples or seams would anyway also interfere with the proper bouncing of the extremely light (2.7 g) ping-pong ball.



The “drag crisis” denotes a precipitous drop in drag on a sphere that happens when the laminar boundary layer turns turbulent, causing the point of separation of the trailing wake (top) to shift rearwards (bottom).

Terminal speed

The variation in drag with Reynolds number makes the calculation of the terminal speed of a spherical ball somewhat more complicated than eq. (19-11). Equating the force of gravity with the drag and eliminating the velocity by means of the Reynolds number we obtain,

$$\text{Re}^2 C_D(\text{Re}) = \frac{8m'g_0}{\pi\rho_{\text{fluid}}\nu^2} = \frac{32}{3} \left(\frac{\rho_{\text{sphere}}}{\rho_{\text{fluid}}} - 1 \right) \frac{a^3 g_0}{\nu^2}, \quad (19-20)$$

where m' is the mass of the sphere reduced by buoyancy. From this equation and a graph of the left hand side, the Reynolds number and thereby the terminal velocity may be determined.

In the limit where the drag coefficient is a constant, we may solve for the terminal speed, which becomes

$$U = \sqrt{\frac{8}{3} \left(\frac{\rho_{\text{sphere}}}{\rho_{\text{fluid}}} - 1 \right) \frac{a g_0}{C_D}}. \quad (19-21)$$

The terminal velocity grows with the squareroot of the density of the sphere, implying that the kinetic energy of the sphere grows with the square of the density. This is why bombs with heavy metal jackets (made, for example, from depleted uranium) are used to penetrate concrete structures and rock.

Example 19.3.1: A skydiver weighing 70 kg curls up like a ball with radius $a = 50$ cm and average density $\rho_{\text{sphere}} \approx 133 \text{ kg m}^{-3}$. Taking $C_D \approx 0.3$ and $\rho_{\text{air}} \approx 1 \text{ kg m}^{-3}$, we obtain $U = 76 \text{ m s}^{-1} = 273 \text{ km h}^{-1}$. The corresponding Reynolds number is $\text{Re} = 4.7 \times 10^6$, confirming the used approximation.

19.4 Beyond spherical shape

The general arguments given in section 19.1 showed that in creeping flow the drag on an arbitrary body is proportional to viscosity, velocity and a shape-dependent factor with dimension of length. Using the Stokes' drag (19-9) as a baseline, we may write the drag on an arbitrary body as

$$\mathcal{D} = 6\pi\eta a_S U, \quad (19-22)$$

where a_S is a characteristic length, sometimes called the *Stokes radius*. The Stokes radius may be determined from a measurement of the terminal speed,

$$a_S = \frac{m'g_0}{6\pi\eta U}, \quad (19-23)$$

where as before m' is the mass of the body corrected for buoyancy.

The Stokes radius may be calculated analytically for some simple bodies, for example a circular disk of radius a . In the two major orientations of the disk, we have

$$\frac{a_S}{a} = \begin{cases} \frac{8}{3\pi} \approx 0.85 & \text{disk orthogonal to flow} \\ \frac{16}{9\pi} \approx 0.57 & \text{disk parallel to flow} \end{cases} \quad (19-24)$$

In spite of the vast differences between the two cases, the Stokes radii are of the same order of magnitude. For general bodies of non-exceptional geometry, one may as a first estimate set the Stokes radius equal some effective radius, determined for example from the surface area or the volume of the body.

At high Reynolds numbers, where viscosity plays a diminishing role, the drag coefficient may as discussed for the sphere be defined to be

$$C_D = \frac{\mathcal{D}}{\frac{1}{2}\rho AU^2}, \quad (19-25)$$

where A is some area that the body presents to the flow. For blunt bodies the area may be taken to be the “shadow” of the body on a plane orthogonal to the direction of motion. For a given shape, the drag force

$$\mathcal{D} = C_D \frac{1}{2} \rho AU^2, \quad (19-26)$$

exposes the dependence on the fluid (ρ), the body size (A), and the state of motion (U). Barring the presence of a drag crisis, typical values for C_D are of the order of unity for bodies of non-exceptional geometry. A flat circular disk orthogonal to the flow has $C_D \approx 1.17$, whereas a circular cup with its opening towards the flow has $C_D \approx 1.4$. If on the other hand the disk is infinitely thin and oriented parallel with the flow, there will be no asymptotic form drag, and the drag coefficient will vanish (as $1/\sqrt{\text{Re}}$) in the limit of infinite Reynolds number.

Drag reduction by *streamlining* is important in the construction of all kinds of moving vehicles, such as cars and airplanes. Car manufacturers have over the years reduced the drag coefficient to lower than 0.4, and there is still room for improvement. In modern times drag-reducing helmets have also appeared on the heads of bicycle racers and speed skaters, giving the performers of these sports quite alien looks. Among animals, drag reduction yields evolutionary advantages, which has led to the beautiful outlines of fast flyers and swimmers, like falcons and sharks. The density of water is about a thousand times that of air, implying a thousand times larger form drag (19-26) in water than in air, although this effect is offset by the higher velocities necessary for flight. This has forced swimming animals towards extremes of streamlined shapes. The mackerel has thus reduced the drag coefficient of its sleek form to the remarkably low value of 0.0043, an order of magnitude lower than for a swimming human [36]. Since muscular power is roughly the same, birds should typically be capable of moving about $\sqrt{1000} \approx 30$ times faster than fish of the same size and shape.

Problems

19.1 Show that for creeping flow we have

$$\nabla^2 p^* = 0 \quad (19-27)$$

$$\nabla^2 \boldsymbol{\omega} = \mathbf{0} \quad (19-28)$$

where $\boldsymbol{\omega} = \nabla \times \mathbf{v}$ is the vorticity field.

* **19.2** Show that the rate of work of the contact forces exerted by a steadily moving body on the fluid through which it moves is $\mathcal{D}U$, where \mathcal{D} is the total drag.

* **19.3** a) Show that the creeping flow solution around a fixed body in an asymptotically uniform steady velocity field \mathbf{U} must be of the form

$$\mathbf{v}(\mathbf{x}) = \mathbf{R}(\mathbf{x}) \cdot \mathbf{U} \quad (19-29)$$

$$p^*(\mathbf{x}) = \eta \mathbf{Q}(\mathbf{x}) \cdot \mathbf{U} \quad (19-30)$$

where $\mathbf{R}(\mathbf{x})$ is a tensor field and $\mathbf{Q}(\mathbf{x})$ is a vector field, both independent of \mathbf{U} .

b) Determine the field equations and the boundary conditions for \mathbf{R} and \mathbf{Q} .

c) Calculate the total force on the body.

19.4 Consider Stokes flow around a sphere of radius a . a) Calculate the volume discharge of fluid passing a concentric annular disk of radius $b > a$ placed orthogonal to the flow. b) Calculate the volume in relation to the volume that would pass through the same disk, if the sphere were not present. c) Justify qualitatively why the ratio vanishes for $b \rightarrow a$.

19.5 Calculate the pressure contribution to the drag from Stokes solution for a sphere.

19.6 Consider spherical Stokes flow and

a) Show that the stream lines are determined by the solutions to

$$\frac{dr}{dt} = v_r = A(r)U \cos \theta$$

$$\frac{d\theta}{dt} = \frac{v_\theta}{r} = -B(r)U \sin \theta$$

with

$$A(r) = 1 - \frac{3a}{2r} + \frac{1a^3}{2r^3} = \left(1 - \frac{a}{r}\right)^2 \left(1 + \frac{1a}{2r}\right)$$

$$B(r) = \frac{1}{r} \left(1 - \frac{3a}{4r} - \frac{1a^3}{4r^3}\right) = \frac{1}{r} \left(1 - \frac{a}{r}\right) \left(1 + \frac{1a}{4r} + \frac{1a^2}{4r^2}\right)$$

b) Show that this leads to a solution of the form

$$\sin \theta = e^{-\int B/A dr} = \frac{d}{(r-a)\sqrt{1+a/2r}} \quad (19-31)$$

where d is an integration constant. This is the align for the streamlines in polar coordinates.

- c) Show that d is the asymptotic distance of the flow line from the polar axis (also called the impact parameter).
- d) Find the relation between d and the point of closest approach of the flow line to the sphere.

19.7 Champagne bubbles of carbon dioxide are typically created at the inner surface of a glass, and later detach due to buoyancy and rise through the liquid which essentially consists of water. Establish a differential equation for the rise of a bubble towards the surface, taking into account buoyancy and viscous friction. You may assume 1) that the bubbles are spherical, 2) that the mass of a bubble is much smaller than the mass of the displaced liquid, 3) that the Reynolds number is small so that buoyancy is always in balance with friction (Stokes flow), 4) that there is no gas exchange with the liquid after the formation of a bubble, and 5) that the expansion of the gas in a bubble is isothermal.

* **19.8 Analytic solution of Stokes flow for a sphere**

- a) Use the field equations and symmetry to show that the solution must be of the form (in spherical coordinates)

$$\mathbf{v}(\mathbf{x}) = a(r)\mathbf{U} + b(r)\mathbf{x}\mathbf{U} \cdot \mathbf{x} , \quad (19-32a)$$

$$p(\mathbf{x}) = \eta c(r)\mathbf{U} \cdot \mathbf{x} , \quad (19-32b)$$

where $a(r)$, $b(r)$, and $c(r)$ are functions only of r .

- b) Use the boundary conditions to show that $a(r)$ and $b(r)$ must vanish at $r = a$, and that at $r \rightarrow \infty$ they satisfy $a(r) \rightarrow 1$ and $r^2 b(r) \rightarrow 0$.
- c) Show that the field equations lead to the ordinary differential equations

$$\frac{d^2 a}{dr^2} + \frac{2}{r} \frac{da}{dr} + 2b = c , \quad (19-33a)$$

$$\frac{d^2 b}{dr^2} + \frac{6}{r} \frac{db}{dr} = \frac{1}{r} \frac{dc}{dr} , \quad (19-33b)$$

$$\frac{1}{r} \frac{da}{dr} + r \frac{db}{dr} + 4b = 0 . \quad (19-33c)$$

- d) Show that these equations are homogeneous in r , and justify that one should look for power solutions

$$a = Ar^\alpha , \quad (19-34a)$$

$$b = Br^\beta , \quad (19-34b)$$

$$c = Cr^\gamma , \quad (19-34c)$$

- e) Show that

$$\beta = \gamma = \alpha - 2 \quad (19-35)$$

and

$$\alpha(\alpha + 1)A + 2B = C , \quad (19-36a)$$

$$(\alpha - 2)(\alpha + 3)B = (\alpha - 2)C , \quad (19-36b)$$

$$\alpha A + (\alpha + 2)B = 0 . \quad (19-36c)$$

f) Show that a non-trivial solution requires

$$(\alpha - 2)\alpha(\alpha + 1)(\alpha + 3) = 0, \quad (19-37)$$

so that the allowed powers are $\alpha = 2, 0, -1, -3$.

g) Show that the most general solution is

$$a(r) = Kr^2 + L + \frac{M}{r} + \frac{N}{r^3}, \quad (19-38a)$$

$$b(r) = -\frac{1}{2}K + \frac{M}{r^3} - 3\frac{N}{r^5}, \quad (19-38b)$$

$$c(r) = 5K + 2\frac{M}{r^3}, \quad (19-38c)$$

where K , L , M , and N are the four integration constants.

h) Show that the boundary conditions at infinity require $K = 0$ and $L = 1$, and that the boundary conditions at $r = a$ require $M = -\frac{3}{4}a$ and $N = -\frac{1}{4}a^3$, leading to the desired solution (19-5).